Detection of a Hard Tail in the X-Ray Spectrum of the Z Source GX 349+2

di Salvo, T.; Robba, N.R.; Iaria, R.; Burderi, L.; Israel, G.; Stella, L.

Published in:
Astrophysical Journal

DOI:
10.1086/321353

THE ASTROPHYSICAL JOURNAL, 554:49–55, 2001 June 10

DETECTION OF A HARD TAIL IN THE X-RAY SPECTRUM OF THE Z SOURCE GX 349+2

T. DI SALVO,[1,2] N. R. ROBBA,[1] R. IARIA,[1] L. STELLA,[3,4] L. BURDERI,[3] AND G. L. ISRAEL[3,4]

Received 2000 November 14; accepted 2001 February 6

ABSTRACT

We present the results of a *BeppoSAX* observation of the Z source GX 349+2 covering the energy range 0.1–200 keV. The presence of flares in the light curve indicates that the source was in the flaring branch during the *BeppoSAX* observation. We accumulated energy spectra separately for the nonflaring intervals and for the flares. In both cases, the continuum is well described by a soft blackbody ($kT_{\rm BB} \sim 0.5$ keV) and a Comptonized spectrum corresponding to electron temperature $kT_e \sim 2.7$ keV, optical depth $\tau \sim 10$ (for a spherical geometry), and seed-photon temperature $kT_{\rm W} \sim 1$ keV. All temperatures tend to increase during the flares. In the nonflaring emission, a hard tail dominates the spectrum above 30 keV. This can be fit by a power law with photon index ~ 2, contributing $\sim 2\%$ of the total source luminosity over the *BeppoSAX* energy range. A comparison with hard tails that are detected in some soft states of black hole binaries suggests that a similar mechanism could originate these components in black hole and neutron star systems.

Subject headings: accretion, accretion disks — stars: individual (GX 349+2) — stars: neutron — X-rays: general — X-rays: stars

1. INTRODUCTION

Low-mass X-ray binaries (LMXBs) are usually divided into Z sources and atoll sources, according to the path they describe in an X-ray color-color diagram or a hardness-intensity diagram (Hasinger & van der Klis 1989). The six known Z sources in the Galaxy are among the most luminous LMXBs and are close to the Eddington limit ($L_{\rm Edd}$) for a 1.4 $M_\odot$ neutron star (NS). The instantaneous position of an individual source in the color-color diagram is an indicator of the mass accretion rate (e.g., Hasinger et al. 1990), which most likely increases along the Z track from the top left to the bottom right.

The LMXBs of the atoll class usually have lower luminosities than the Z sources [generally in the range $(0.01–0.1)L_{\rm Edd}$]. These sources can be found in soft or hard states (see Barret et al. 2000). In the hard state, their spectrum is dominated at high energies by a power law, sometimes showing an exponential cutoff at energies of $\gtrsim 100$ keV (see, e.g., Barret et al. 2000, and references therein). On the other hand, the spectrum of the Z sources is much softer, with cutoff energies usually well below 10 keV. However, hard tails were occasionally detected in their spectra. The first detection was in the spectrum of Sco X-1. Besides the main X-ray component, at a temperature of ~ 4 keV, Peterson & Jacobson (1966) found a hard component dominating the spectrum above 40 keV. The latter component was observed to vary by as much as a factor of 3. Since then, hard tails were repeatedly searched for in the spectrum of Sco X-1 and other Z sources; they were detected on occasion (e.g., Buselli et al. 1968; Riegler, Boldt, & Serlemitsos 1970; Agrawal et al. 1971; Haymes et al. 1972), but in most cases they were not found, perhaps owing to pronounced variations (e.g., Miyamoto & Matsuoka 1977, and references therein; Soong & Rothschild 1983; Jain et al. 1984; Ubertini et al. 1992). Recently a hard tail was detected in another Z source, GX 17+2, observed by *BeppoSAX* in a broad energy range (0.1–200 keV). In this case, the intensity variations of the hard tail were clearly correlated to the source's spectral state: a factor of 20 decrease was observed moving from the horizontal branch (HB) to the normal branch (NB; Di Salvo et al. 2000). The presence of a variable hard tail in Sco X-1 was confirmed by OSSE and *RXTE* observations (Strickman & Barret 2000; D'Amico et al. 2000). A hard tail was also detected in Cir X-1 (Iaria et al. 2001) and in type II bursts from the Rapid Burster (Masetti et al. 2000).

GX 349+2, also known as Sco X-2, is one of the six known Z sources. Similar to the case of Sco X-1, GX 349+2 possesses a short and underdeveloped HB (if at all). The source variability in the frequency range below 100 Hz is closely correlated to the source position on the X-ray color-color diagram, as in other Z sources. Twin quasi-periodic oscillations at kHz frequencies were detected in the upper and middle NB (Zhang, Strohmayer, & Swank 1998). In this paper we report the results of a spectral study of GX 349+2 in the energy range 0.1–200 keV based on data obtained with *BeppoSAX*. This led to the detection of a hard component fitted by a power law with photon index ~ 1.8 or by a thermal bremsstrahlung with $kT \sim 120$ keV.

2. OBSERVATIONS AND ANALYSIS

The Narrow Field Instruments (NFI) on board *BeppoSAX* are four co-aligned instruments that cover more than 3 decades in energy, from 0.1 keV up to 200 keV, with good spectral resolution over the whole range (see Boella et al. 1997a for a detailed description of *BeppoSAX* instruments). The instruments are as follows: a Low Energy Concentrator Spectrometer (LECS; a thin-window, position-sensitive proportional counter with extended low-energy response, 0.1–10 keV; Parmar et al. 1997), two Medium Energy Concentrator Spectrometers (MECS; position-sensitive proportional counters operating in the 1.3–10 keV band; Boella et al. 1997b), a High Pressure Gas

[1] Dipartimento di Scienze Fisiche ed Astronomiche, Università di Palermo, via Archirafi 36, 90123 Palermo, Italy; disalvo@gifco.fisica.unipa.it.

[2] Astronomical Institute Anton Pannekoek, University of Amsterdam and Center for High-Energy Astrophysics, Kruislaan 403, NL 1098 SJ Amsterdam, The Netherlands.

[3] Osservatorio Astronomico di Roma, Via Frascati 33, 00040 Monteporzio Catone, Roma, Italy; stella@coma.mporzio.astro.it.

[4] Affiliated with the International Center for Relativistic Astrophysics.

Scintillation Proportional Counter (HPGSPC; energy range 7–60 keV; Manzo et al. 1997), and a Phoswich Detection System (PDS; energy range 13–200 keV; Frontera et al. 1997).

GX 349+2 was observed by *BeppoSAX* from 2000 March 10 20:42 UT to March 11 23:10 UT, with an effective exposure time of ∼16 ks in the LECS, ∼45 ks in the MECS, ∼45 ks in the HPGSPC, and ∼22 ks in the PDS. We selected the data for scientific analysis in circular regions centered on the source with 8′ and 4′ radius for LECS and MECS, respectively. The background subtraction was obtained with standard methods by using blank sky observations. The background subtraction for the high-energy (non-imaging) instruments was obtained by using off-source data for the PDS and Earth-occultation data for the HPGSPC. There is no evidence indicating the presence of contaminating sources in the fields of view (FOVs) of the HPGSPC and PDS, in either the on-source or the off-source positions. In fact, the off-source PDS count rates are in the expected range, and the HPGSPC and PDS spectra align well with each other and the MECS spectra.

Relative normalizations of the four NFIs were treated as free parameters in the model fitting, except for the MECS normalization, which was fixed to a value of 1. We checked after the fitting procedure that these normalizations were in the standard range for each instrument.[5] The energy ranges used in the spectral analysis were 0.12–4 keV for the LECS, 1.8–10 keV for the MECS, 8–40 keV for the HPGSPC, and 15–200 keV for the PDS. We rebinned the energy spectra in order to have approximately the same number of bins per resolution element of the instrument across the entire energy range. Moreover, a 1% systematic error was applied to all these spectra in order to take into account calibration residuals.

In Figure 1 we show the 200 s binned MECS light curve of GX 349+2 in the 1.8–10 keV range. A flare lasting ∼4 ks is clearly apparent close to the beginning of the observation, followed by a series of smaller flares. In Figure 2*a* we show the color-color diagram of GX 349+2, where we define the hard color (HC) as the ratio of the counts in the 7–10.5 keV to the 4.5–7 keV energy bands and the soft color (SC) as the ratio of the counts in the 4.5–7 keV to the 1.8–4.5 keV bands. The SC and HC relationship versus the source intensity in the 1.8–10.5 keV is also shown in Figure 2*b* (*upper and lower panel*, respectively). The color variations in these diagrams are mainly caused by the spectral changes associated with the flares, during which both the HC and the SC increase. In consideration of the presence of fairly large flares in the light curve and the shape of the source variations in the color-color diagram, we identify the state of the source with the flaring branch (FB) of the Z path. Hints of the NB/FB vertex are visible in the diagrams at SC ∼ 0.2 and HC ∼ 0.3. We extracted energy spectra during the nonflaring intervals, corresponding to an SC lower than 0.48, and during the flares, corresponding to an SC higher than 0.48.

We tried several two-component models to fit the source X-ray spectrum during the nonflaring state. In particular, to describe the softer component we tried a blackbody or a disk-multicolor blackbody (*diskbb* in XSPEC; Mitsuda et al. 1984); to describe the harder component we tried blackbody or Comptonization models such as a power law with high-energy exponential cutoff, *compst* (Sunyaev & Titarchuk 1980), *comptt* (Titarchuk 1994), and *pexriv* (i.e., a power law with exponential cutoff with its reflection component; Magdziarz & Zdziarski 1995). None of these models could well describe the source X-ray spectrum in the whole *BeppoSAX* energy range because an excess of emission was present above ∼30 keV (see Fig. 3*a*, *upper and middle panels*). We then considered the low-energy part (0.1–30 keV) of the spectrum, where we obtained the best fit by using a blackbody plus *comptt* for the continuum; this model gave a reduced χ^2 of $\chi^2_r = 1.19$, while we obtained χ^2_r from 1.49 to 2.35 for the other models we fitted. An emission line at ∼6.7 keV and an edge at ∼8.5 keV, probably produced by highly ionized iron, are also necessary (probabilities of chance improvement of the fit are less than 10^{-20} and $\sim 8.6 \times 10^{-5}$ for the addition of an emission line and an absorption edge, respectively). The fit is further improved by the addition of a low-energy Gaussian emission line at ∼1.16 keV (chance probability of $\sim 7 \times 10^{-9}$).

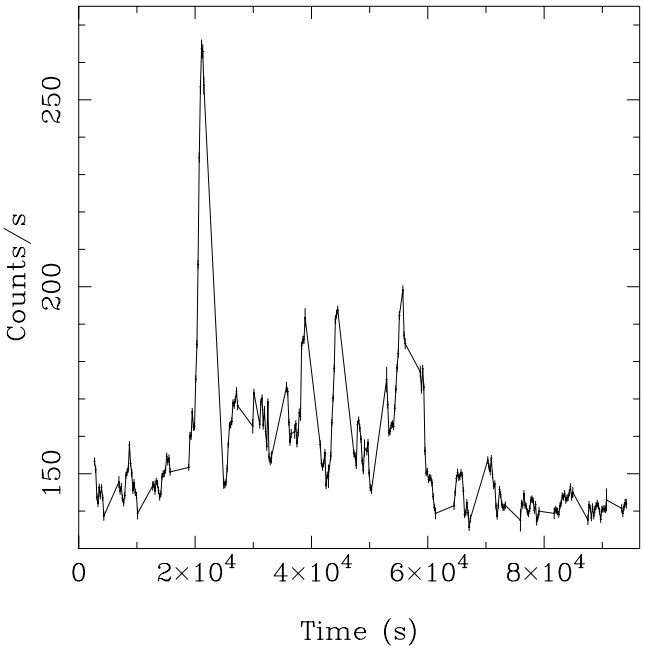

FIG. 1.—Light curve of GX 349+2 in the 1.8–10 keV energy range (MECS data). Each bin corresponds to 200 s integration time.

A two-component continuum model was not sufficient to be well fit to the nonflaring spectrum in the whole *BeppoSAX* range. A hard excess is clearly visible above 30 keV with respect to any of the two-component models that we tried. For example, the best-fit model described above, when fitted in the whole 0.1–200 keV range, gives rise to the residuals (in units of σ) shown in Figure 3*a* (*middle panel*). A significant improvement of the fit was obtained by adding to the model a power law with photon index ∼1.9, which eliminates the residuals at high energies (see Fig. 3*b*, *lower panel*). With the addition of this component, the χ^2 decreases from 397 (for 191 degrees of freedom) to 220 (189 dof). An *F*-test indicates that the probability of chance improvement is negligibly small. The contribution of this power-law component to the unabsorbed 0.1–200 keV luminosity is ∼2%. Alternative models for the hard excess cannot be excluded. Using a thermal brems-

[5] See the *BeppoSAX* handbook at http://www.sdc.asi.it/software/index.html.

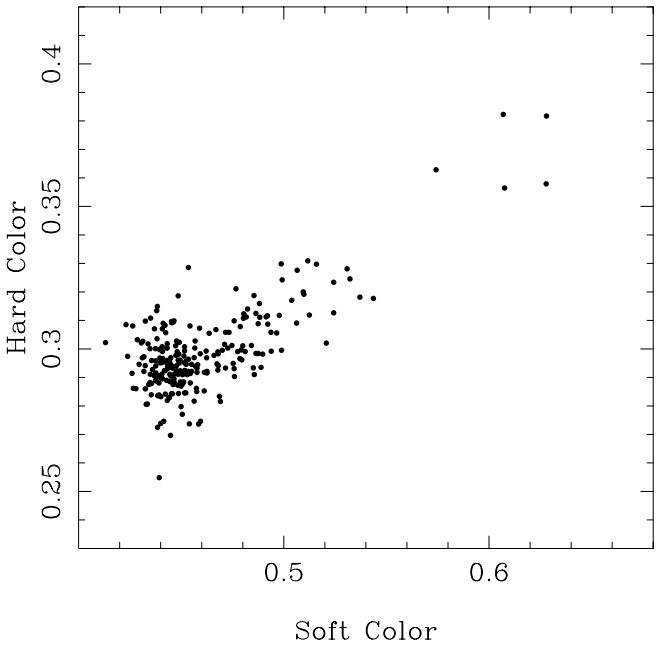

FIG. 2a

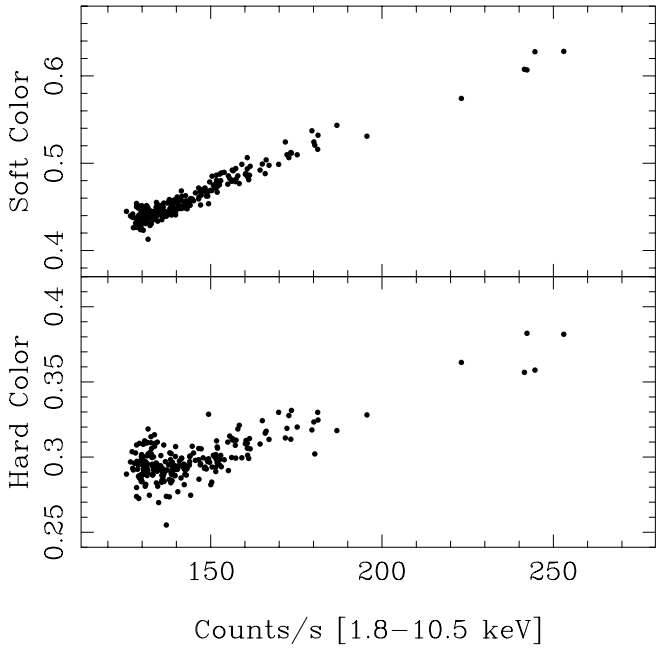

FIG. 2b

FIG. 2.—(*a*) Color-color diagram of GX 349+2. The hard color is the ratio of the counts in the 7–10.5 keV and the 4.5–7 keV energy bands, and the soft color is the ratio of the counts in the 4.5–7 keV and 1.8–4.5 keV energy bands. Each bin corresponds to 200 s. (*b*) Soft color (*upper panel*) and hard color (*lower panel*) vs. the source count rate in the MECS (energy range 1.8–10.5 keV).

strahlung for the hard component, we obtain a similarly good fit for a temperature of $kT_{TB} = 120 \pm 50$ keV. A high-energy power-law spectrum might in principle be produced by Comptonization of seed photons with a blackbody distribution in an optically thin, hot region. Therefore, we also tried to fit the hard component using the Comptonization model *compbb* (Nishimura, Mitsuda, & Itoh 1986), which, however, gave a worse fit. In particular, we substituted the blackbody plus power law of the best-fit model with *compbb*, obtaining a $\chi^2_r = 1.41$ (for 189 dof) and a temperature of the optically thin Comptonizing region higher than 150 keV. The high χ^2_r is caused by large residuals (up to 4–5 σ) in the energy range above $\sim$70 keV because of a sharp cutoff in the model, which is not present in the data. In other words, because these data do not show a high-energy cutoff in the *BeppoSAX* range, this implies a high electron temperature ($\gtrsim$100 keV) or a nonthermal origin.

TABLE 1

RESULTS OF FITTING OF GX 349+2 SPECTRA IN THE 0.12–200 keV ENERGY BAND[a]

Parameter	Nonflaring	Flare
N_H ($\times 10^{22}$ cm^{-2})	$0.66^{+0.03}_{-0.02}$	0.64 ± 0.3
kT_{BB} (keV)	0.51 ± 0.01	0.59 ± 0.02
R_{BB} (km)	36 ± 2	31 ± 2
kT_W (keV)	1.03 ± 0.03	1.37 ± 0.04
kT_e (keV)	2.65 ± 0.05	2.95 ± 0.07
τ	11.7 ± 0.4	10.5 ± 0.5
R_W (km)	8.8 ± 0.6	7.0 ± 0.5
Photon index	$1.9^{+0.4}_{-0.3}$	1.9 (fixed)
Power law N	$3^{+9}_{-2} \times 10^{-2}$	$<2.3 \times 10^{-2}$
E_{Fe} (keV)	6.73 ± 0.05	6.73 (fixed)
σ_{Fe} (keV)	0.31 ± 0.08	0.31 (fixed)
I_{Fe} ($\times 10^{-3}$ photons cm^{-2} s^{-1})	8.8 ± 1.5	8.5 ± 3.7
Fe equivalent width (eV)	71	34
E_{line} (keV)	1.16 ± 0.03	...
σ_{line} (keV)	0.05 ± 0.05	...
I_{line} ($\times 10^{-2}$ photons cm^{-2} s^{-1})	$1.9^{+0.8}_{-0.5}$	...
Emission-line equivalent width (eV)	17	...
E_{edge} (keV)	8.9 ± 0.2	...
τ_{edge} ($\times 10^{-2}$)	4 ± 1	...
Flux (ergs cm^{-2} s^{-1})	1.91×10^{-8}	3.26×10^{-8}
χ^2_{red} (dof)	1.17 (189)	1.22 (119)

[a] The model consists of a blackbody, a Comptonized spectrum modeled by *comptt*, a power law, two Gaussian emission lines, and an absorption edge. Uncertainties are 90% confidence level for a single parameter of interest. The power-law normalization is in units of photons keV^{-1} cm^{-2} s^{-1} at 1 keV. The total unabsorbed flux is in the 0.1–200 keV energy range. The effective exposure time was a factor of $\sim$20 larger in the nonflaring spectrum than in the flaring.

No useful LECS data were obtained during the flares because of the low exposure time; owing to UV-contamination problems, the LECS is usually operated only at satellite nighttime, resulting in a much reduced on-source time, and therefore low-energy data (0.1–1.8 keV) were not available in this case. The spectrum during the flare cannot be described by a single component such as a blackbody or a *comptt*. As in the case of the nonflaring spectrum, we obtained a good fit using a blackbody plus *comptt* model. The addition of an iron line with centroid energy and width fixed to the best-fit values found in the nonflaring spectrum gave an improvement of the fit at 99.9% confidence level. On the other hand, the addition of a power law at high energies did not improve the fit: the χ^2 decreases from 145 (for 119 dof) to 144 (118 dof), which is clearly not significant. To study the variation of the power-law intensity with respect to the nonflaring spectrum, we fixed the photon index to the best-fit value of 1.9 found in the nonflaring spectrum and calculated the corresponding power-law normalization. We find an upper limit (at 90% confidence level) on the power-law unabsorbed 0.1–200 keV flux of 3.6×10^{-10} ergs cm^{-2} s^{-1} ($\sim$1% of the unabsorbed 0.1–200 keV flux during the flare). Therefore we conclude

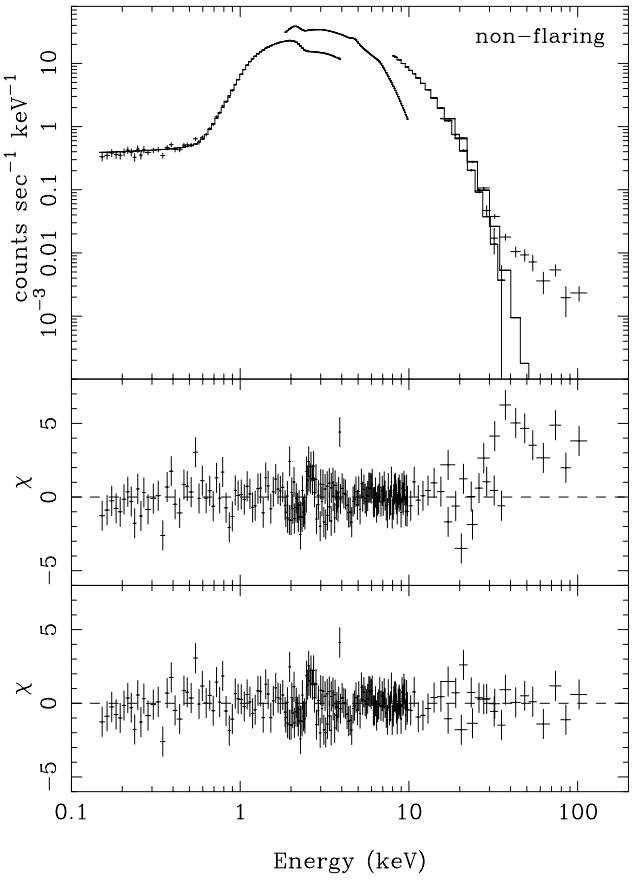

FIG. 3*a*

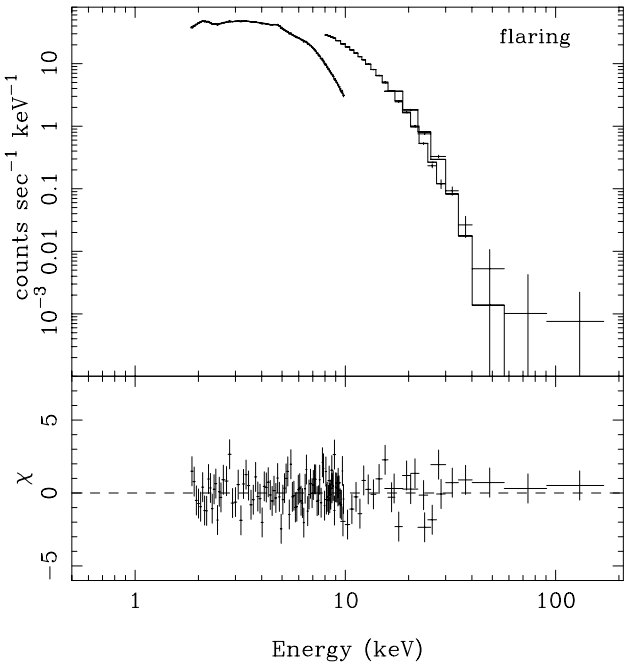

FIG. 3*b*

FIG. 3.—(*a*) Broadband spectrum of GX 349+2 during the nonflaring emission together with the best-fit two-component continuum model (blackbody plus *comptt*, *upper panel*) and the corresponding residuals in units of σ (*middle panel*). Residuals in units of σ (*lower panel*) with respect to the best-fit model reported in Table 1, including a power-law hard component. (*b*) GX 349+2 spectrum during flaring intervals together with the best-fit model (*upper panel*) and residuals in units of σ (*lower panel*).

that there is evidence that the hard component weakens during the flare, although the upper limit is still compatible with the best-fit power-law normalization during the nonflaring emission.

We report in Table 1 the best-fit parameters corresponding to the spectra during the nonflaring and flaring intervals. These spectra are shown in Figures 3*a* and 3*b* (*top panels*, respectively) together with the residuals with respect to the best-fit models (*bottom panels*). The unfolded spectra are also shown in Figures 4*a* and 4*b*, respectively, together with the components of the best-fit models reported in Table 1.

3. DISCUSSION

We fitted the *BeppoSAX* energy spectra of GX 349+2, extracted at different positions of the source in the color-color diagram. The best-fit model up to energies of $\sim$30 keV consists of a blackbody and a Comptonization spectrum (described by the *comptt* model), two emission lines, and an absorption edge. The blackbody is at temperature $kT_{\rm BB} \sim 0.5$–0.6 keV, and the radius of the (spherical) blackbody-emitting region is $R_{\rm BB} \sim 35$ km (using a distance of 5 kpc; Cooke & Ponman 1991; Christian & Swank 1997). The temperature of the soft seed photons for the Comptonization is $kT_{\rm W} \sim 1$ keV. These photons are Comptonized in a hotter ($kT_e \sim 3$ keV) region of moderate optical depth ($\tau \sim 10$–12 for a spherical geometry). The radius of the region emitting the seed-photon Wien spectrum, calculated as in In't Zand et al. (1999), is

$$R_{\rm W} = 3 \times 10^4 D \sqrt{f_{\rm bol}/(1+y)}/(kT_{\rm W})^2 \text{ km} \approx 7\text{–}9 \text{ km}, \quad (1)$$

where D is the distance in kpc, $f_{\rm bol}$ is the bolometric flux in ergs cm^{-2} s^{-1}, and $kT_{\rm W}$ is in keV. A broad ($\sim$0.7 keV FWHM) iron Kα emission line is present at $\sim$6.7 keV, with equivalent width $\sim$30–70 eV, accompanied by an absorption edge at $\sim$8.5 keV. The high energy of both the line and the edge indicates that these features are produced in a highly ionized region (corresponding approximately to Fe XXV). We also found evidence for an emission line at $\sim$1.2 keV, with equivalent width of $\sim$20 eV, which can be associated with emission from the L shell of Fe XXIV or, perhaps, the K shell of Ne X (see, e.g., Kallman et al. 1996). We note that the main differences in the continuum below 30 keV between the spectra during the flares and the nonflaring emission are in the temperatures of the blackbody and Comptonized components; both temperatures are higher during the flares than during the nonflaring emission, while the optical depth of the Comptonized component is smaller during the flares. The iron emission line remains approximately unchanged.

A hard component is required to match the spectrum above 30 keV during the nonflaring emission. This component can be fit by a power law with photon index $\sim$2, contributing $\sim$2% of the 0.1–200 keV source flux. This component is not required in the flare spectrum, where it probably weakens, contributing a smaller fraction of the source flux. Evidence for such a hard component was previously found in this source by the *Ariel V* satellite (Greenhill et al. 1979) and was fit by a thermal spectrum with $kT \sim 30$ keV. In our data this component is much harder, corresponding to a temperature of $\sim$120 keV. We note that the high-energy instrument on board *Ariel V* had

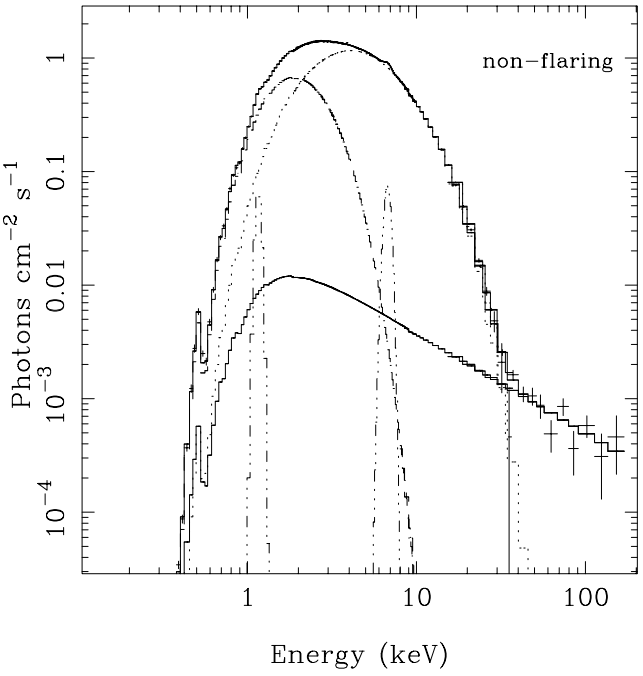

FIG. 4*a*

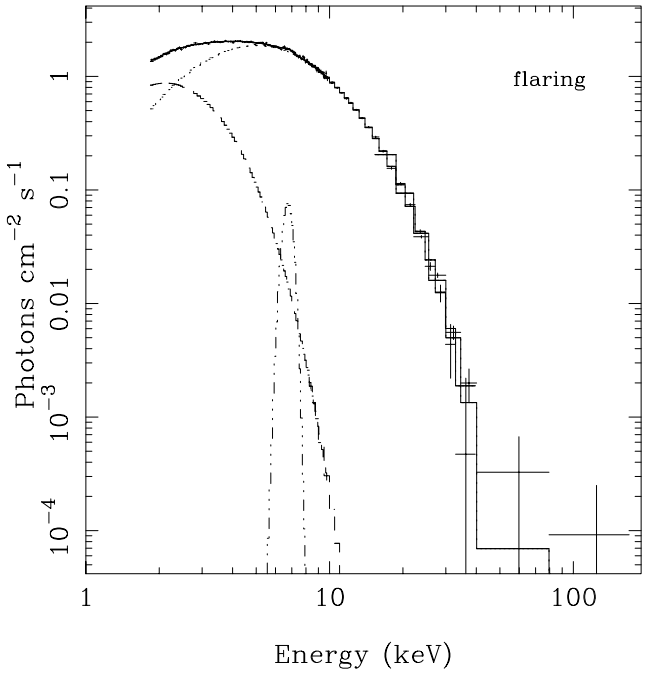

FIG. 4*b*

FIG. 4.—(*a*) Unfolded spectrum of the GX 349+2 nonflaring emission and the best-fit model of Table 1, shown in this figure as the solid line on top of the data. The individual model components are also shown, namely the blackbody (*dashed line*), the Comptonized spectrum (*comptt* model, *dotted line*), two Gaussian emission lines at ~1.2 keV and ~6.7 keV (*triple-dot–dashed lines*), and the power law (*solid line*). (*b*) Unfolded spectrum of the GX 349+2 flaring emission and the best-fit model of Table 1, shown as the solid line on top of the data. The components of the model are also shown, namely the blackbody (*dashed line*), the *comptt* model (*dotted line*), and a Gaussian emission line at ~6.7 keV (*triple-dot–dashed line*).

a field of view of 8° FWHM, much larger than the PDS field of view.

The smaller PDS field of view, 1°.3 FWHM, reduces the possibility of the presence of contaminating sources. The eclipsing binary system 4U 1700−37 (the only nearby X-ray source brighter than 1 μJy; see, e.g., Valinia & Marshall 1998) is 1°.4 away from GX 349+2 and is out of the PDS field of view. Another possible contaminating source is the hard diffuse emission of the Galactic ridge. Using data from Valinia & Marshall (1998), for latitudes $1^\circ.5 < |b| < 4^\circ$ and longitudes $|l| < 15^\circ$ (the region of GX 349+2), the flux of the diffuse Galactic emission is $\sim 3.2 \times 10^{-11}$ ergs cm^{-2} s^{-1} in the 10–60 keV energy range for the effective solid angle of the PDS FOV. This is 1 order of magnitude lower than the flux of the hard power-law component we detected from GX 349+2 in the same energy range. Given the flux of the power-law component in the 13–80 keV energy range, which is $\sim 1.2 \times 10^{-10}$ ergs cm^{-2} s^{-1}, we calculated the probability of finding an active galactic nucleus in the PDS FOV at a flux level equal to or higher than $\sim 1.2 \times 10^{-10}$ ergs cm^{-2} s^{-1}. We find a small probability of $\sim 2 \times 10^{-3}$ (see F. Fiore & F. Tamburelli 2000, in preparation; Levine et al. 1984). We can also exclude the possibility that this hard component is an instrumental feature because in other *BeppoSAX* observations of soft sources there was no evidence of a hard excess. A clear example of this is given by the *BeppoSAX* spectrum of GX 17+2 in the lower NB (Di Salvo et al. 2000). We find that a power law with photon index 1.9, like that detected in this paper, is incompatible with those data, which give a 90% upper limit on the power-law unabsorbed 0.1–200 keV flux of 2.5×10^{-11} ergs cm^{-2} s^{-1}. It is therefore plausible that this hard component represents emission from GX 349+2.

A similar hard component has also been observed in other Z sources, indicating that this is probably a common feature of these sources. The presence (or strength) of these components appears to be related to the source state or to its position in the color-color diagram. In a *Ginga* (1.5–38 keV energy range) observation of GX 5−1, a hard excess was detected (Asai et al. 1994).[6] This component was fit by a power law with photon index 1.8 (Asai et al. 1994), and its intensity decreased from the NB to the FB, i.e., from low to high mass accretion rate. In a *BeppoSAX* observation of GX 17+2, the hard component (power-law photon index of ~2.7) was detected in the HB, and its intensity significantly decreased in the NB (Di Salvo et al. 2000). Cir X-1, thought to be a peculiar Z source (Shirey et al. 1998), was observed by *BeppoSAX* in the FB (Iaria et al. 2001). Also in this case a hard tail was detected in the nonflaring spectrum. We note that the hard component detected here in GX 349+2 is one of the hardest among the high-energy components detected so far in bright LMXBs. It corresponds to a photon index of ~1.9, with no evidence of a high-energy cutoff in the *BeppoSAX* range. In fact, using thermal models to fit to it, we obtain electron temperatures $\gtrsim 100$ keV. The power-law tail observed in the NB of GX 5−1 (Asai et al. 1994), had a photon index of ~1.8, similar to the one we measured for GX 349+2. Also, Cir X-1 showed a spectral state similar to that of GX 349+2 observed here (Iaria et al. 2001). However, in Cir X-1 the power law was much steeper (photon index ~3.3) than in the case of GX 349+2, and the low-energy continuum was also characterized by a softer electron tem-

[6] Note, however, that the detection of a hard tail from GX 5−1 was not confirmed by SIGMA observations (Barret & Vedrenne 1994).

perature of the Comptonized component, $\lesssim 1$ keV. In all these cases the hard component seems to become weaker for higher accretion rates (see also Fig. 5), while the relative contribution of the hard component to the flux in a given source state appears to be different in different sources. Yet, in recent *RXTE*/HEXTE observations of Sco X-1, a hard power-law tail was detected in 5 out of 16 observations, without any clear correlation to position in the color-color diagram (D'Amico et al. 2000).

It is already known that some atoll sources, the so-called X-ray bursters, can show a hard component in their spectra, which is similar to that observed in the spectra of accreting black holes (BH). Given that BHs and NSs are hardly distinguishable by their broadband spectral shape (see also Barret et al. 2000 and references therein), Barret, McClintock, & Grindlay (1996) introduced another criterion based on the comparison of hard and soft luminosities. Plotting the 1–20 keV luminosity versus the 20–200 keV luminosity for BHs and NSs of the atoll class, they observed that all NS systems in which a hard component had been detected lie in the so-called X-ray burster box, while all BH systems lie outside of it (see Fig. 5). If we plot the luminosities of the Z sources GX 17+2 (Di Salvo et al. 2000), Cir X-1 (Iaria et al. 2001), and GX 349+2 in the same diagram, we find that these data lie clearly outside of the X-ray burster box, and there is no clear distinction between Z sources and BHs (Fig. 5). Stated differently, this result shows that BHs are

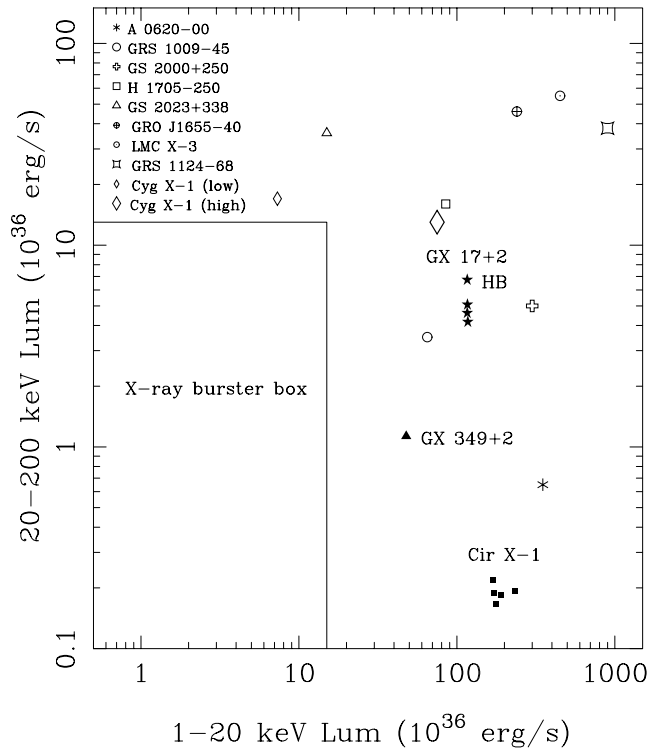

FIG. 5.—20–200 keV vs. 1–20 keV luminosities of BH binaries (*open symbols*; Barret et al. 2000) and NS type Z binaries (*filled symbols*). The so-called X-ray burster box is plotted as a solid line. Its boundaries are defined as in Barret et al. (2000).

not the only sources to possess high-energy tails when their 1–20 keV luminosity exceeds $\sim 1.5 \times 10^{37}$ ergs s^{-1}. In particular, the hard components in Z sources seem to be similar to the extended power-law tails detected in the so-called very high state (and perhaps intermediate state) of Galactic BH systems (e.g., Grove et al. 1998). On the other hand, it appears to be still true that only BHs can emit bright hard X-ray tails, with a 20–200 keV luminosity $\gtrsim 1.5 \times 10^{37}$ ergs s^{-1}. This might be related to the higher Eddington luminosity that on average characterizes BHs. The fact that the luminosity in the hard tail observed in Z sources is similar in terms of Eddington luminosity to that seen in BHs is further evidence suggesting that probably the same mechanism originates the hard tails in both BHs and NSs. This would imply that this mechanism does not depend on the presence or absence of a solid surface.

As in BHs, the hard tails observed in Z sources can be produced either in a thermal or nonthermal corona (e.g., Poutanen & Coppi 1998) or in a bulk motion of matter close to the NS (e.g., Titarchuk & Zannias 1998; Papathanassiou & Psaltis 2001). Fast radial converging motions are unlikely to be dominant in the innermost region of the accretion flow in such high-luminosity systems because of the strong radiation pressure emitted from (or close to) the NS surface. However, power-law tails, dominating the spectra at high energy, can also be produced when the flows are mildly relativistic ($v/c \sim 0.1$) or when the velocity field does not converge (Psaltis 2001). Therefore, azimuthal motions around the NS or outflows can be the probable origin of these components, with flatter power laws corresponding to higher optical depth of the scattering medium and/or higher bulk electron velocities, in a way that is similar to thermal Comptonization (see Psaltis 2001). It has been proposed that nonthermal high-energy electrons, responsible for the hard tails observed in Z sources, might originate in a jet (Di Salvo et al. 2000; Iaria et al. 2001; see also Fender 2001 for a review regarding both BH and NS systems). In fact, all the Z sources are detected as variable radio sources, with the highest radio fluxes associated with the HB. The radio emission weakens in the NB and is not detected any longer in the FB (Hjellming & Han 1995; Fender & Hendry 2000, and references therein). This hypothesis is in agreement with the behavior of GX 17+2, where the hard tail was observed in the HB. In GX 349+2 the hard tail is present at the NB/FB vertex, where the radio flux should be near its minimum and probably weakens when the source moves further into the FB. However, note that a similar correlation was not observed in the case of Sco X-1 (D'Amico et al. 2000). Further observations will help clarify the correlation between hard X-ray and radio emission in these sources.

The authors thank D. Barret and L. Titarchuk for interesting discussions. This work was supported by the Italian Space Agency (ASI) and by the Ministero della Ricerca Scientifica e Tecnologica (MURST).

REFERENCES

Agrawal, P. C., et al. 1971, Ap&SS, 10, 500
Asai, K., et al. 1994, PASJ, 46, 479
Barret, D., McClintock, J. E., & Grindlay, J. E. 1996, ApJ, 473, 963
Barret, D., Olive, J. F., Boirin, L., Done, C., Skinner, G. K., & Grindlay, J. E. 2000, ApJ, 533, 329
Barret, D., & Vedrenne, G. 1994, ApJS, 92, 505
Boella, G., Butler, R. C., Perola, G. C., Piro, L., Scarsi, L., & Blecker, J. 1997a, A&AS, 122, 299
Boella, G., et al. 1997b, A&AS, 122, 327
Buselli, G., Clancy, M. C., Davison, P. J. N., Edwards, P. J., McCracken, K. C., & Thomas, R. M. 1968, Nature, 219, 1124
Christian, D. J., & Swank, J. H. 1997, ApJS, 109, 177
Cooke, B. A., & Ponman, T. J. 1991, A&A, 244, 358
D'Amico, F., Heindl, W. A., Rothschild, R. E., & Gruber, D. E. 2001, ApJ, 547, L147
Di Salvo, T., et al. 2000, ApJ, L544, 119
Fender, R. P. 2001, in AIP Conf. Proc., Int. Symp. on High Energy Gamma-Ray Astronomy, ed. F. Aharonian & H. Voelk (New York: AIP), in press (astro-ph/0101233)
Fender, R. P., & Hendry, M. A. 2000, MNRAS, 317, 1
Frontera, F., et al. 1997, A&AS, 122, 357
Greenhill, J. G., Coe, M. J., Burnell, S. J. B., Strong, K. T., & Carpenter, G. F. 1979, MNRAS, 189, 563
Grove, J. E., Johnson, W. N., Kroeger, R. A., McNaron-Brown, K., Skibo, J. G., & Phlips, B. F. 1998, ApJ, 500, 899
Hasinger, G., & van der Klis, M. 1989, A&A, 225, 79
Hasinger, G., van der Klis, M., Ebisawa, K., Dotani, T., & Mitsuda, K. 1990, A&A, 235, 131
Haymes, R. C., Harnden, F. R., Johnson, W. N., Prichard, H. M., & Bosch, H. E. 1972, ApJ, 172, L47
Hjellming, R. M., & Han, X. H. 1995, in X-Ray Binaries, ed. W. H. G. Lewin, J. van Paradijs, & E. P. J. van den Heuvel (Cambridge Astrophys. Ser.; Cambridge: Cambridge Univ. Press), 308
Iaria, R., Burderi, L., Di Salvo, T., La Barbera, A., & Robba, N. R. 2001, ApJ, 547, 412
In't Zand, J. J. M., et al. 1999, A&A, 345, 100
Jain, A., et al. 1984, A&A, 140, 179
Kallman, T. R., Liedahl, D., Osterheld, A., Goldstein, W., & Kahn, S. 1996, ApJ, 465, 994
Levine, A. M., et al. 1984, ApJS, 54, 581
Magdziarz, P., & Zdziarski, A. A. 1995, MNRAS, 273, 837
Manzo, G., Giarrusso, S., Santangelo, A., Ciralli, F., Fazio, G., Piraino, S., & Segreto, A. 1997, A&AS, 122, 341
Masetti, N., et al. 2000, A&A, in press (astro-ph/0009044)
Mitsuda, K., et al. 1984, PASJ, 36, 741
Miyamoto, S., & Matsuoka, M. 1977, Space Sci. Rev. E, 20, 687
Nishimura, J., Mitsuda, K., & Itoh, M. 1986, PASJ, 38, 819
Papathanassiou, H., & Psaltis, D. 2001, MNRAS, in press (astro-ph/0011447)
Parmar, A. N., et al. 1997, A&AS, 122, 309
Peterson, L. E., & Jacobson, A. S. 1966, ApJ, 145, 962
Poutanen, J., & Coppi, P. S. 1998, Phys. Scr., T77, 57
Psaltis, D. 2001, ApJ, in press (astro-ph/0011534)
Riegler, G. R., Boldt, E., & Serlemitsos, P. 1970, Nature, 266, 1041
Shirey, R. E., Bradt, H. V., Levine, A. M., & Morgan, E. H. 1998, ApJ, 506, 374
Soong, Y., & Rothschild, R. E. 1983, ApJ, 274, 327
Strickman, M., & Barret, D. 2000, in AIP Conf. Proc. 510, 5th Compton Symp., Detections of Multiple Hard X-Ray Flares from Sco X-1 with OSSE, ed. M. L. McConnel & J. M. Ryan (New York: AIP), 222
Sunyaev, R. A., & Titarchuk, L. G. 1980, A&A, 86, 121
Titarchuk, L. 1994, ApJ, 434, 570
Titarchuk, L., & Zannias, T. 1998, ApJ, 493, 863
Ubertini, P., Bazzano, A., Cocchi, M., La Padula, C., & Sood, R. K. 1992, ApJ, 386, 710
Valinia, A., & Marshall, F. E. 1998, ApJ, 505, 134
Zhang, W., Strohmayer, T. E., & Swank, J. H. 1998, ApJ, 500, L167